Kriging Water Levels with a Regional-Linear and Point-Logarithmic Drift

by Matthew J. Tonkin[1] and Steven P. Larson[1]

Abstract

Ground water levels measured in the vicinity of pumping wells are kriged using a regional-linear and point-logarithmic drift, the latter derived from the approximation to the Theis equation for drawdown in response to a pumping well. Kriging is widely used throughout the hydrogeologic discipline, most commonly as the preferred method for constructing gridded hydrogeologic datasets suitable for contouring. Residuals arising from using the most common (linear) drift to krige water levels in the vicinity of extraction wells often indicate large local departures from the linear drift, which correlate with areas of drawdown. The combined regional-linear and point-logarithmic drift accounts for these drawdowns using a logarithmic approximation for the curvature of the potentiometric surface. The drift model approximates the principal physical processes that govern ground water flow and ultimately govern the autocorrelation of ground water elevation data. This approach produces maps of contoured water levels that more realistically represent physical conditions and allow for improved interpretation of measured water-level data by including features and information known to be present. Additional benefits include an improved estimate of the regional (background) hydraulic gradient and generation of an approximately flow-conserved grid suitable for two-dimensional particle tracking.

Introduction

Kriging is widely used throughout the hydrogeologic discipline as the preferred method for constructing gridded hydrogeologic datasets suitable for contouring. Kriging was introduced as a least-squares estimator that improved on methods such as distance weighting or polynomial interpolation for which weighting was a determinant (Delhomme 1978). An advantage of kriging is that, in the absence of measurement error, it is an exact interpolator at measurement points. In addition, kriging yields both estimated values and estimate variances (Skrivan and Karlinger 1977). Kriging is ideally an investigative and iterative process, including development and fitting of an analytical function representing the underlying trend or drift where evidence exists for such, and development of a semivariogram to describe the pattern of residuals (measured data minus drift) (Volpi and Gambolati 1978). This universal kriging approach is not typically adopted for gridding ground water level data. Despite the extensive literature that discusses kriging, calculating custom drift functions is not a straightforward matter, and standard approaches rarely extend beyond linear and polynomial drift models (Chiles and Delfiner 1999). In areas of fairly uniform regional hydraulic gradients, the linear drift can improve the aesthetics of a contour map. However, visual inspection of contours generated in this manner indicates that the linear drift does not produce a surface that is adequately close to conserving flow in areas of localized discharge or recharge.

As a consequence, interpretation of water levels constructed without a drift model or using a linear drift is typically limited to broad features, such as principal direction(s) of flow and areas of significant drawdown or mounding. Although this capability can be improved by increasing the number and density of monitoring wells—provided the wells are suitably located—water-level monitoring budgets rarely allow for a network sufficient for accurately representing the curvature of the potentiometric surface near extraction wells. Such a network is particularly important in downgradient areas where constraint of the capture zone by determination of the stagnation zone can be critical. All of these factors make contouring of measured ground water elevations typically unsuitable for delimiting the capture zone of a pumping well.

An approach for gridding ground water level data is presented here. Application of this method produces contoured data maps that can improve interpretation of measured water-level data. A combined regional-linear and point-logarithmic drift is employed to specifically account for drawdown and mounding in the vicinity of extraction and injection wells using a logarithmic approximation for the curvature of the potentiometric surface. The point-logarithmic drift is derived from the approximation to the Theis equation for drawdown due to a pumping well. Examples are provided comparing contoured ground water levels measured in the vicinity of pumping wells, kriged using no-drift, linear-drift, and the new combined drift models. Data requirements for the new method are limited to knowledge of pumping activities, including location and rates, and knowledge of the geographic coordinates of monitoring wells. Primary benefits from application of this method include improved estimates of the regional (background) hydraulic gradient and generation of a gridded dataset suitable for two-dimensional particle tracking.

[1]S.S. Papadopulos and Associates Inc., 7944 Wisconsin Ave., Bethesda, MD 20814; (301) 718-8900; fax (301) 718-8909; Matt@SSPA.com, SPL@SSPA.com

Received April 2001, accepted November 2001.

Inclusion of a logarithmic component in the drift model for kriging water-level data has been previously proposed but, to our knowledge, not presented (Volpi and Gambolati 1978). The approach presented here arose without knowledge of this prior study and, it is hoped, complements and extends the discussion presented therein with some examples.

Drift Model

Kriging using a drift or trend model, termed "universal kriging," is typically performed where a smoothly varying trend is present in the data. The drift component is usually modeled as a function of the data coordinates, whose unknown parameters are fitted from the data (Deutsch and Journel 1998). The underlying model is then the sum of the drift component plus the residuals:

$$Z(u) = m(u) + R(u) \quad (1)$$

where

$Z(u)$ = value of random or regionalized variable
$m(u)$ = drift (trend)
$R(u)$ = residual component
u = Cartesian coordinate location (x,y) for two-dimensional kriging.

The residual component is typically modeled as a zero-mean stationary random function (RF) (Deutsch and Journel 1998).

A linear drift is defined as the least-squares fit of the planar surface, described by

$$\text{Linear drift} = A + BX + CY \quad (2)$$

where X is x (or easterly) coordinate (dimension of length [L]); Y is y (or northerly) coordinate (L); and A, B, and C are fitted parameters of the drift model calculated from the data.

The kriging algorithm identifies the least-squares fit of the drift model to the data, assuming that residuals R(u) are uncorrelated (Deutsch and Journel 1998).

The Theis equation for drawdown in response to pumping can be approximated using (Ferris et al. 1962; Rouse 1949)

$$s = \frac{Q}{4\pi T} \ln\left(\frac{2.25Tt}{r^2 S}\right) \quad (3)$$

where

Q = pumping rate at extraction well (L^3T^{-1})
S = aquifer storage (−)
T = aquifer transmissivity (L^2T^{-1})
s = drawdown of the potentiometric surface (L)
r = radial distance to the pumping well (L)
t = time since pumping began (T)
π = ~ 3.14159
ln = natural logarithm.

Equation 3 describes a logarithmic cone of depression, centered on the extraction well. This can be rewritten as

$$s = \frac{Q}{4\pi T}\left[\ln\left(\frac{2.25Tt}{S}\right) + \ln\left(\frac{1}{r}\right)^2\right] = \frac{Q}{4\pi T}\left[\ln\left(\frac{2.25Tt}{S}\right) + 2\ln\left(\frac{1}{r}\right)\right] \quad (4)$$

At any time when the change in hydraulic gradients is zero, the first term in Equation 4 can be considered a constant, and the drawdown at a monitoring well is inversely proportional to the logarithm of the radial distance of the monitoring well from the extraction well, proportional to the pumping rate Q and inversely proportional to the transmissivity (T). Combining Equations 2 and 4, the drift (termed "linear-log" in the following discussion) is described by

$$\text{Drift}_{ij} = A + BX + CY - \frac{Q}{2\pi T}\ln(r) \quad (5)$$

Because the transmissivity is assumed constant throughout the aquifer, the relative magnitude of drawdown at a monitoring well due to pumping at multiple extraction wells is determined only by Q and r. Using the principle of superposition, the drawdown due to pumping of up to n extraction or injection wells can be summed, i.e.,

$$s_{ij} = -\sum_{1}^{n} Q_n \ln(r_n) \quad (6)$$

Where s_{ij} is the drawdown at location (i, j)(L); Q_n is the pumping rate at the nth extraction well (L^3T^{-1}); r_n is the radial distance of extraction well Q_n from location (i, j)(L); and (i, j) may represent (row, column) grid location or Cartesian coordinates.

The complete linear-log drift is then invoked in the kriging routine as

$$\text{Drift}_{ij} = A + BX + CY + s_{ij} \quad (7)$$

By including the logarithmic component, the drift model approximates the principal physical processes that govern ground

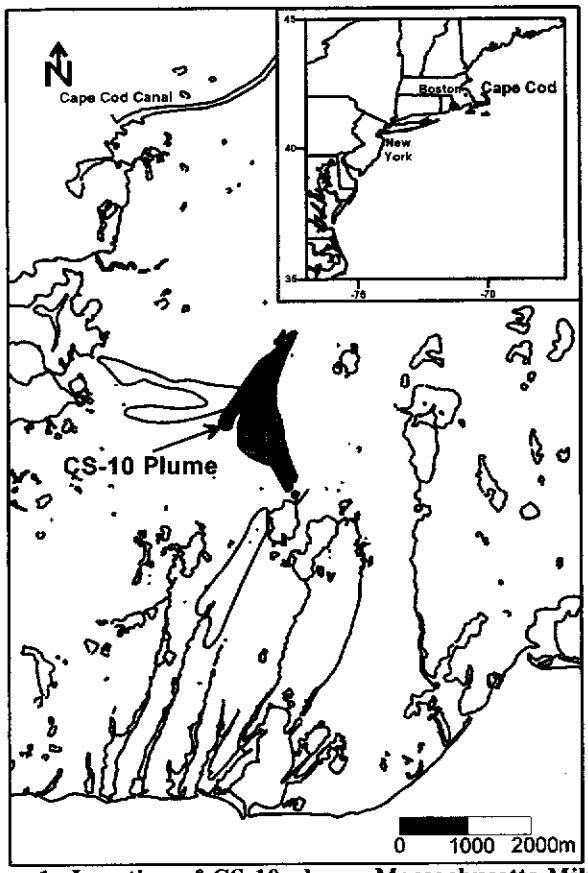

Figure 1. Location of CS-10 plume, Massachusetts Military Reservation, Cape Cod.

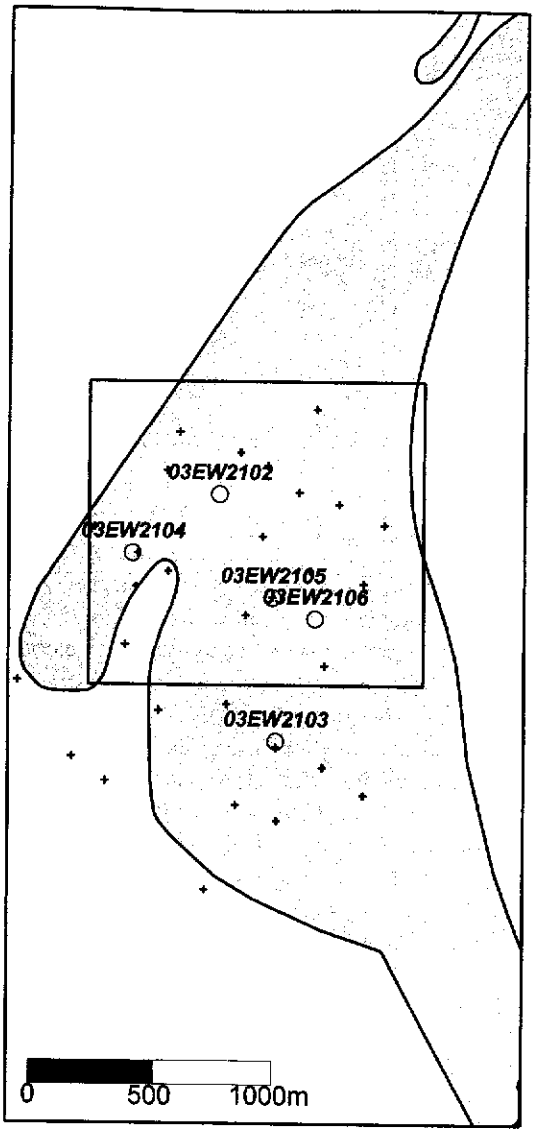

Figure 2. Location of monitoring and extraction wells of the CS-10 plume, and the local area of well-capture estimation.

water flow and ultimately govern the autocorrelation of ground water elevation data. Accordingly, assumptions underlying the Theis equation are implicit in the kriging routine, principally (Rouse 1949):

- The pumping well penetrates and receives water from the entire saturated thickness of the aquifer.
- The aquifer is confined; if the aquifer is unconfined, drawdowns should be less than ~10% of the saturated thickness of the aquifer.
- The aquifer is homogeneous, isotropic, and of infinite areal extent.
- The drawdown and/or mounding has reached a steady-state condition. If this is not the case, the rate of change in hydraulic gradients should approach zero.

Because the form of the underlying drift is assumed to apply to the entire dataset, the drift model parameters are calculated from a global estimation of Z(u). Linear-log kriging is performed using a selection of Fortran routines modified from U.S. Geological Survey Program Number K603, coded by Skriven and Karlinger (1977).

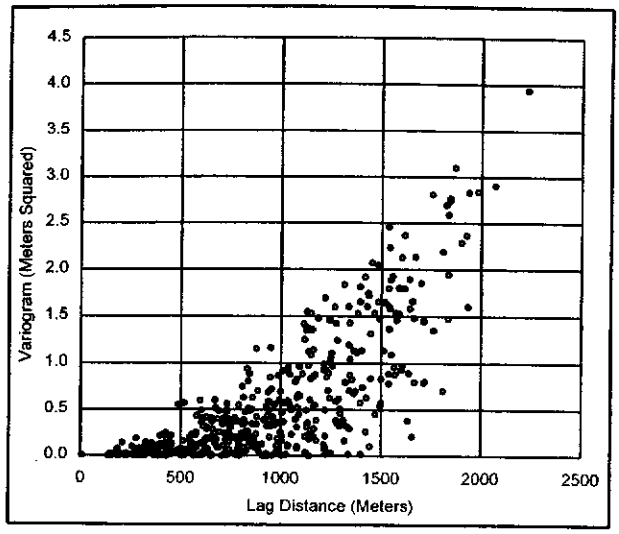

Figure 3. Measured data (raw) semivariogram.

Example Dataset: Cape Cod, Massachusetts

Water levels measured in 32 wells of the Chemical Spill-10 (CS-10) plume, Massachusetts Military Reservation (MMR), Cape Cod (Figure 1) monitoring well network were gridded using the approach detailed previously. Numerous excellent discussions of remedial activities at MMR are available in the literature, e.g., AFCEE (2000) and the MMR Web site at www.mmr.org. The principal contaminants in the CS-10 plume are trichloroethene (TCE) and perchloroethene (PCE), and the selected remedy for the plume is pump and treat. The CS-10 plume is within the Mashpee Pitted Plain (MPP) sediments, which comprise well to poorly sorted, fine- to coarse-grained sands forming a broad outwash plain that typically displays high hydraulic conductivities on the order of 2×10^{-4} m/sec (15 m/day) or greater (Hess et al. 1992). Drawdowns resulting from pumping of CS-10 extraction wells typically do not exceed 1 to 1.5 m of a total saturated thickness averaging 60 m. Assumptions underlying the Theis approximation are considered to be fairly well adhered to.

Water levels selected for this study were measured in 1999 at wells in the upgradient area of the plume, where four extraction wells were being operated to remove ground water contaminated with TCE and PCE. The monitoring network in this area is fairly dense, with monitoring well separations on the order of a few tens to a few hundred meters. Nineteen monitoring wells in the middle of the study area are shown in Figure 2; the remaining wells lie to the south and west of this local-scale map. Water-level contours are shown only for the "zoom" area because this is the area of interest for determining extraction well-capture zones. At the time water levels were collected for this study, two extraction wells had monitoring wells within 20 m for use in aquifer tests. For the remaining extraction wells, the nearest monitoring wells were ~150 m away. In the case of one extraction well (03EW2102), the water level in the nearest monitoring well was not measured, and the nearest water-level measurement was at a distance of ~300 m. The raw data semivariogram is shown in Figure 3. The parabolic behavior of the raw semivariogram is a strong diagnostic indicator of the existence of a trend in the data (Clark and Harper 2000).

Initially, point kriging was performed for a regular grid of 200×200 points, spaced on a 7×7 m grid, assuming no drift, a linear drift, and a linear-log drift. In each case, a linear semivariogram

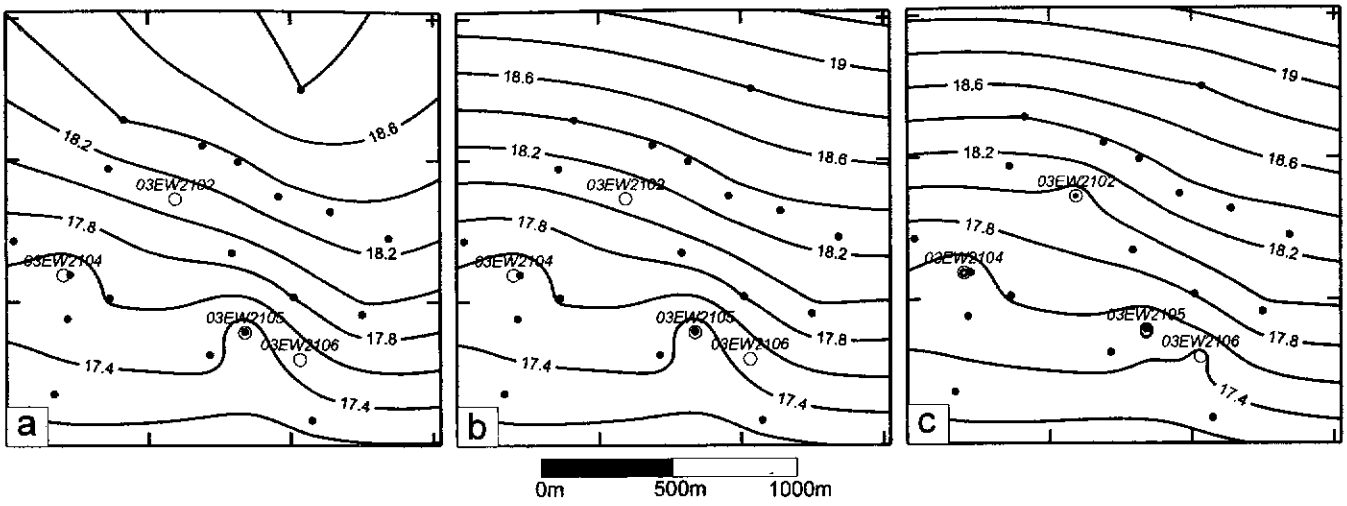

Figure 4. Comparison of ground water contours: (a) no-drift, (b) linear-drift, and (c) linear-log drift.

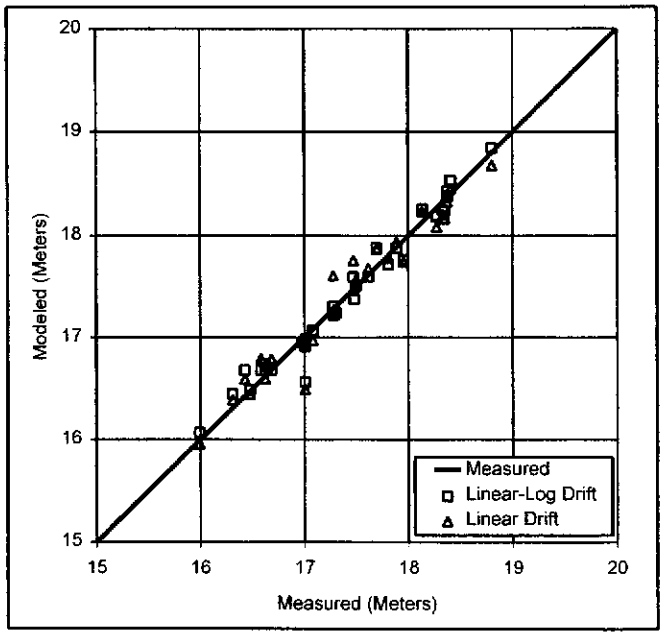

Figure 5. Calculated versus measured water level for linear and linear-log drifts.

was used. Visual comparison of the ground water contours on the three resulting maps (Figure 4) indicates:

1. In areas of high data control (closely spaced monitoring wells) and low stress (far from pumping), contours of the no-drift, the linear-drift, and linear-log maps are similar.
2. In areas of high data control (closely spaced monitoring wells) and high stress (close to pumping), the contours of the no-drift and linear-drift maps are similar; however, contours of the linear-log map exhibit the more defined structure of the underlying drift model.
3. In areas of low data control, contours of the no-drift, linear-drift, and linear-log maps differ markedly. In particular, contours of the no-drift map converge in the north of the domain where a single data point is present, resulting in an unrealistic map of the ground water surface.

As the distance from measurement points increases, the underlying drift dominates the contour pattern, and further differences between the linear and linear-log drift maps are apparent. Water-level contours constructed using the linear-log drift are concave to the extraction wells for some distance away from each extraction well. The concavity decreases with distance from each extraction well. This pattern is expected due to drawdown in response to pumping. Water-level contours calculated using the linear drift are concave close to each extraction well, but the concavity is less defined farther from the wells, and the contours display the underlying linear drift. This comparison suggests that kriging with a linear drift may result in a poor approximation of the underlying trend or regional gradient. Although the scattergrams are at first glance indistinguishable (Figure 5), on closer inspection, the linear-log drift estimates (squares) are typically closer to the line of equality than the linear-drift estimates (circles). This condition occurs largely from systematic (typically by design) bias in the location of monitoring wells close to extraction and injection wells and the tendency of the universal kriging routine to spread residuals (error) from the drift calculation throughout the gridded domain. The sum of squared differences for the two models differs by ~50%—in this case, 0.5 m^2 for the linear-log drift model and 0.78 m^2 for the linear-drift model.

The gridded ground water levels calculated with no-drift, the linear-drift, and the linear-log drift formed the basis of particle-tracking analyses using Path3D (Zheng 1992) to delineate the well-capture zones (Figure 6). The saturated thickness was simulated for a confined, single layer, isotropic homogeneous aquifer of 60 m. Comparison of the resulting maps indicates:

1. In areas of high data control and low stress (consistent gradients), particle tracks are similar.
2. In areas of high data control and a single stress (e.g., in the area of steep gradients close to 03EW2104), particle tracks of the linear and linear-log drift maps are quite similar.
3. In areas of fairly high data control and more than one stress (e.g., in the area of complex gradients close to 03EW2105 and 03EW2106), the linear and linear-log drift particle tracks differ markedly. In particular, the capture zone of 03EW2105 appears grossly exaggerated in the linear drift map because the data density is insufficient to account for the complex shape of the ground water surface near two extraction wells.
4. In areas of low data control, near single or multiple stresses, the linear and linear-log drift particle tracks differ markedly. In particular, near 03EW2102 and 03EW2106, the linear drift map shows no drawdown, and consequently, no particles are

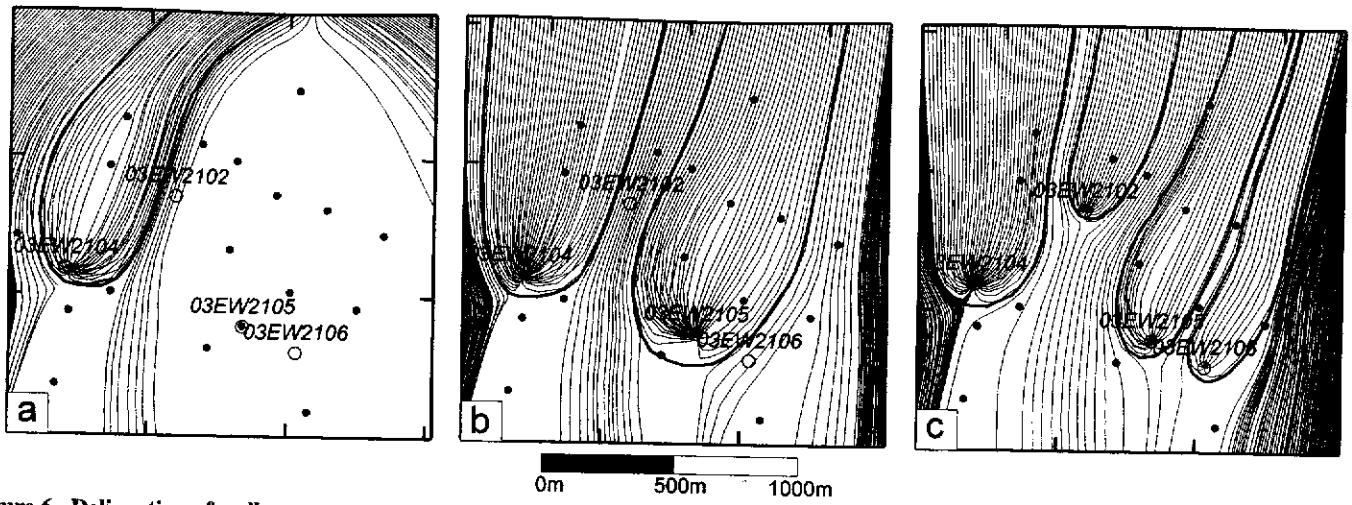

Figure 6. Delineation of well-capture zones by particle-tracking analyses: (a) no-drift, (b) linear-drift, and (c) linear-log drift.

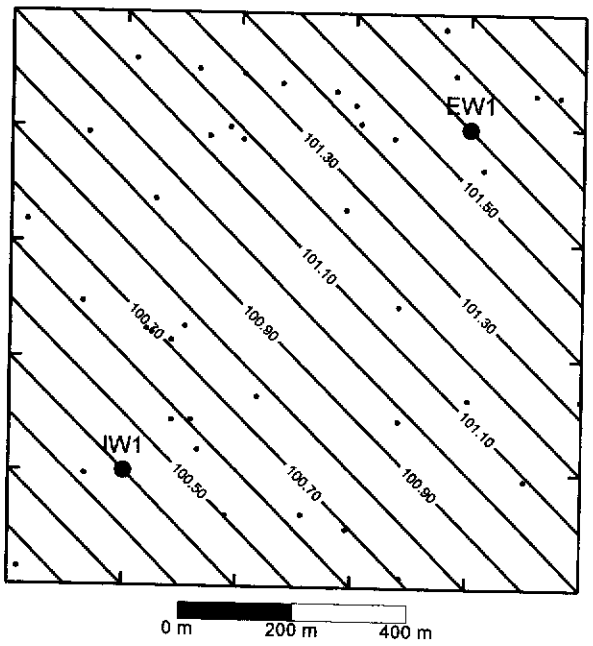

Figure 7. Example of well arrangement and uniform regional gradient.

removed at these sinks. This situation contradicts operations and maintenance information indicating that these wells were operating at their design extraction rates.

In this example, the linear-log drift generated a gridded dataset that is more representative of the physical conditions expected in the modeled domain and suitable for particle-tracking analysis for preliminary estimates of well-capture zones. This improvement arises largely from the closer approximation of conserved flow conditions calculated with the linear-log drift and provides a defensible basis for using the gridded surface to conduct particle-tracking analyses. Deviations from conserved flow are largely determined by the magnitude and distribution of residuals from the linear-log drift model and violations of assumptions underlying the Theis approximation.

Analysis of the effects of grid discretization on estimation of well-capture zones using the linear-log method is not entered into here. These can be expected to be comparable to those effects arising in two-dimensional finite difference ground water modeling, as described by Zheng (1994). In general, "ideal" grid dis-

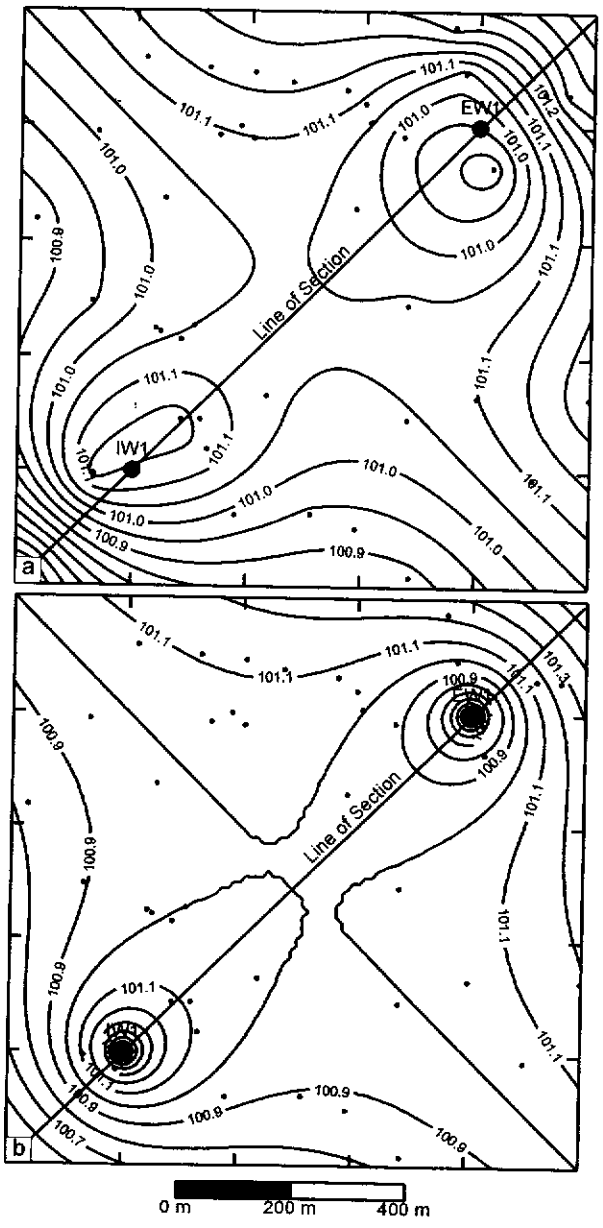

Figure 8. Ground water elevation contours calculated from linear and linear-log drift models.

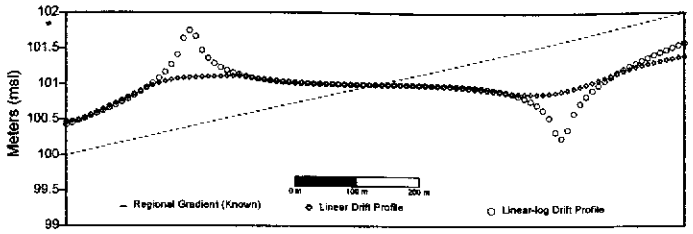

Figure 9. Profile of regional hydraulic gradients calculated from linear and linear-log drift models.

cretization is proportional to the magnitude of the source(s) and sink(s) simulated and, in this respect, is case specific.

Regional Hydraulic Gradient

Accurate estimates of the background, or regional, gradient are particularly important where compliance objectives for pump-and-treat systems include restrictions on gradient changes outside the impacted area. A linear drift can be considered as a least-squares fit of a planar surface to the ground water levels. To reduce the overall error throughout the gridded domain, the kriging routine may calculate an unrealistic underlying trend that is biased by the location of monitoring wells near pumping wells. By way of example, Figure 7 shows an artificially generated uniform background potentiometric surface. The area of interest is 1000×1000 m. Superimposed on this surface are (1) a well extracting 3.15×10^{-2} m^3/sec in the northeast (upgradient) quadrant, and (2) a well injecting 3.15×10^{-2} m^3/sec in the southwest (downgradient) quadrant. The underlying uniform hydraulic gradient, from northeast to southwest, was generated with the equation

$$h_{ij} = 100 + 0.001X + 0.001Y \quad (8)$$

where h is the elevation at location (i, j); X is the x coordinate; and Y is the y coordinate.

The resultant ground water elevation is then

$$h_{ij} = 100 + 0.001X + 0.001Y + s_{ij} \quad (9)$$

where s_{ij} is the net drawdown/mounding at (i, j) in response to pumping.

Ground water elevations were calculated at 40 imaginary monitoring wells within the domain, the locations of which were generated from a two-variable uniform random field. Drawdown and mounding at each point was calculated using Equation 4. Ground water elevation contours were then constructed by gridding the water levels at these 40 points, using the linear and linear-log drift models. Because this imaginary dataset is constructed using the theory explicit in the linear-log drift model, the linear-log kriging routine can be expected to exactly represent the structure present. Perhaps the most notable difference is that, in the linear-drift figure, the centers of highest drawdown and mounding are removed from the extraction and injection wells, respectively (Figure 8). This effect would be overcome by measuring water levels in the extraction and injection wells. However, water levels measured in pumping wells are often unrepresentative of levels in the formation adjacent to the well screen due to well losses. This circumstance is particularly evident in injection wells that have suffered severe fouling and resultant loss of efficiency.

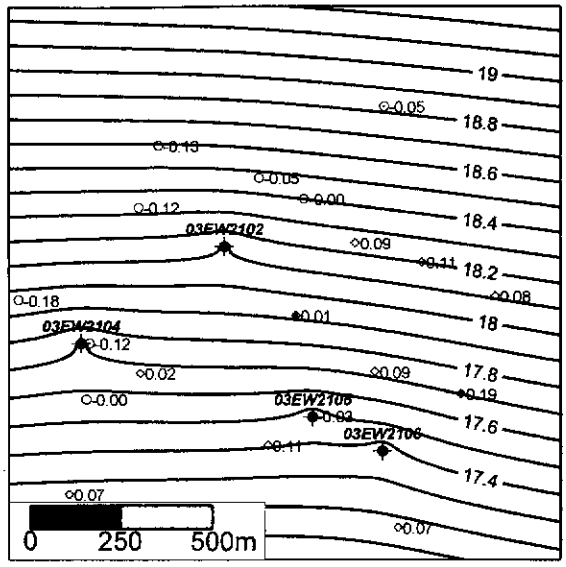

Figure 10. Contour map of linear-log drift model and posted residuals.

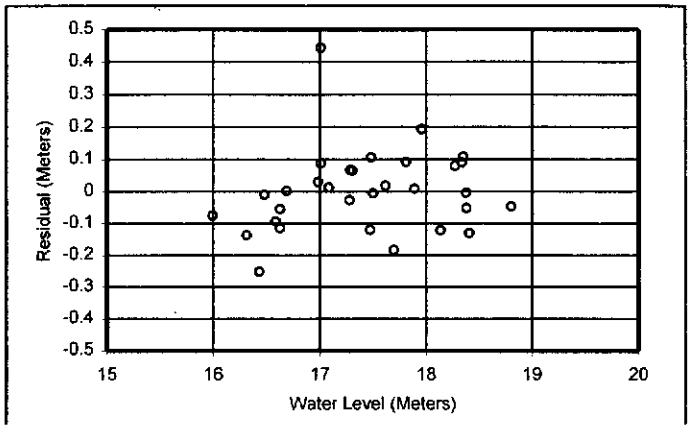

Figure 11. Residual versus water level, Cape Cod dataset.

In profile, the calculated surfaces differ markedly (Figure 9). The surface generated from the linear-drift model is perhaps best described as muted. In the area upgradient (northeast) of the extraction well and downgradient (southwest) of the injection well, the slope diverges from the known uniform background gradient. Alternatively, the surface generated from the linear-log model displays the characteristic cones of impression and depression around the injection and extraction well, respectively; at the margins of the gridded domain, the slope is converging asymptotically (logarithmically) on the uniform background gradient. Because the combined regional-linear and point-logarithmic drift specifically accounts for the drawdown and mounding, distribution of the residual error throughout the domain does not significantly affect the calculated background hydraulic gradient. The coefficients of the fitted linear drift surface (Equations 7 and 8) are 100.88 (A), 0.00045 (B), and 0.00043 (C) m, respectively—here the gradient coefficients B and C are ~50% of the known gradient coefficients.

Residual Error and Semivariogram Selection

Sources of residual error fall into two broad categories: measurement error and model error (which includes deviations of the test data from model assumptions). This paper does not include a rigorous investigation of error because the primary intention is to

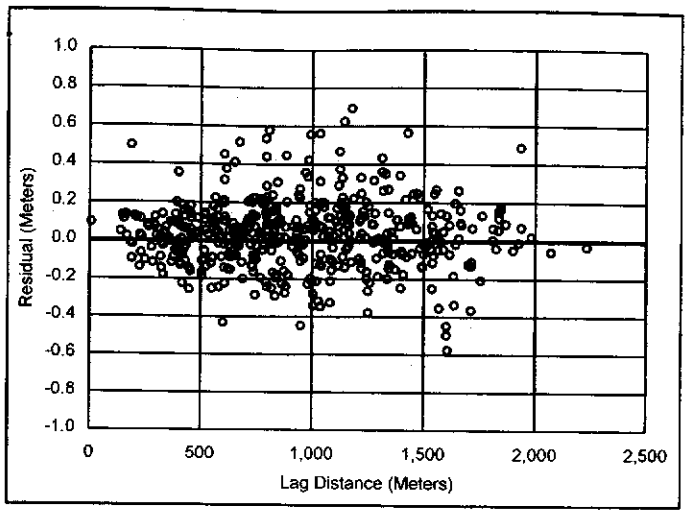

Figure 12. Residual versus lag-distance for paired monitoring points, Cape Cod dataset.

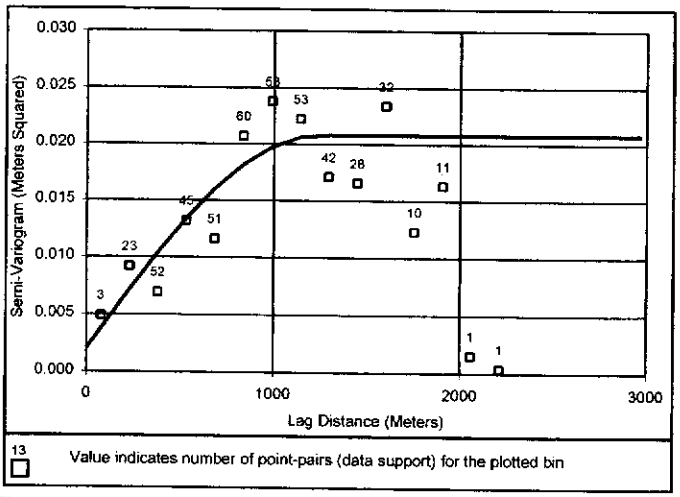

Figure 13. Calculated semivariogram of residuals from linear-log drift model.

outline some clear advantages of the linear-log approach. To accomplish this, a comparative analysis of model suitability and accuracy is provided.

As indicated previously, drift model parameters are calculated from a global estimation of Z(u). The spatial distribution of residuals is perhaps best appreciated using a horizontal (pure nugget) semivariogram, contouring the drift model and posting the residuals. This approach is possible because, although kriging is an exact interpolator at the measured data locations, point kriging at estimation locations removed from the data eliminates discontinuities at the measured data locations and provides a map of the least-squares drift model surface. This realization is presented for the linear-log model (Figure 10) but not the linear-drift model, which is simply a uniform gradient from north-northeast to south-southwest.

For the Cape Cod dataset, the residuals do not appear closely related to water level (Figure 11) or lag distance (Figure 12), nor is any residual trend or global correlation structure immediately apparent. This result is expected because estimation of the trend surface assumes the residuals to be uncorrelated. At first glance, a dilemma may appear unavoidable when selecting a suitable semivariogram model; however, residuals can be expected to show local correlation. The calculated semivariogram for the residuals from the linear-log drift is presented as Figure 13, together with an example spherical model (bin-width = 150 m). This semivariogram plot spans the entire dataset and was constructed using equi-width bins such that the number of point-pairs (i.e., weight or support) representing each plotted point varies greatly. Plotted values for separation distances greater than 1650 m are supported by fewer than 15 point-pairs; in particular, the last two are each supported by only one point-pair. Beyond this distance, the combined impact of lack of support and boundary effects render the semivariogram untenable. This supports the conclusion that the covariance is typically not well known (or estimatable) beyond one-half the field size (Deutsch and Journel 1998), and hence that the "best" results should be achieved using a semivariogram addressing only half the field size and a search-radius of one-quarter the field size. For the Cape Cod dataset, wells to the southeast may be affected by ground water extraction activities several thousand meters to the southwest that are not explicitly included in the drift model used.

For the Cape Cod dataset, the most visually appealing results are achieved using a short-range linear or spherical semivariogram to describe the near-field variance. Maps of grids created with default horizontal (i.e., the drift), linear, and spherical residual semivariograms are presented for comparison (Figure 14). The linear and spherical-model semivariogram maps are quite similar in appearance, which is probably because the spherical semivari-

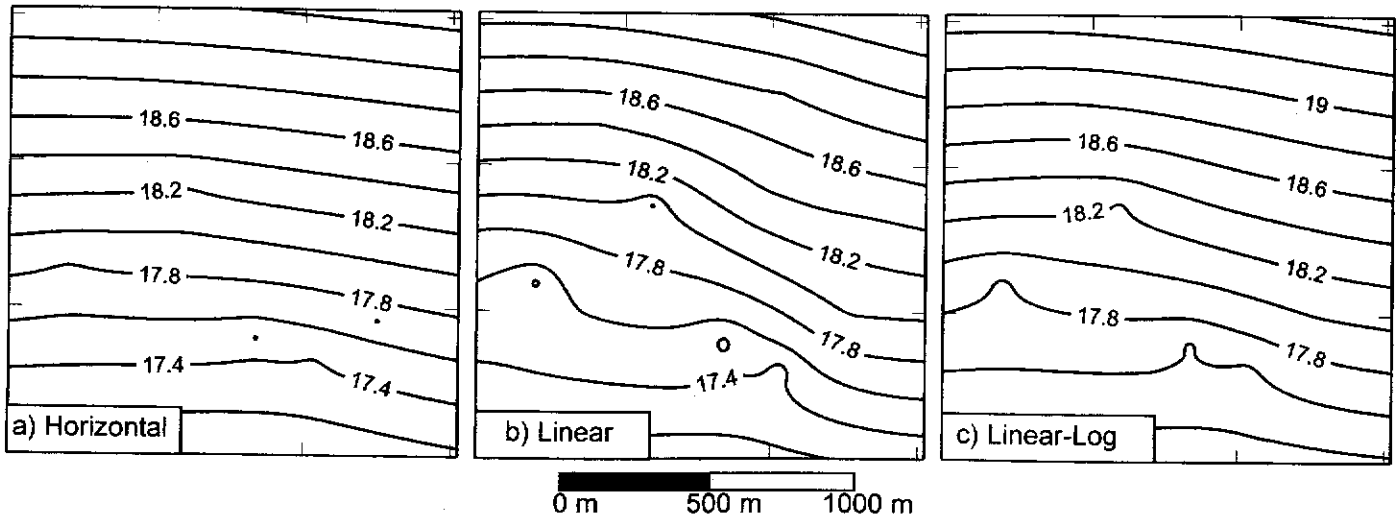

Figure 14. Water-level contours constructed with (a) horizontal, (b) linear, and (c) spherical semivariograms in addition to the linear-log drift.

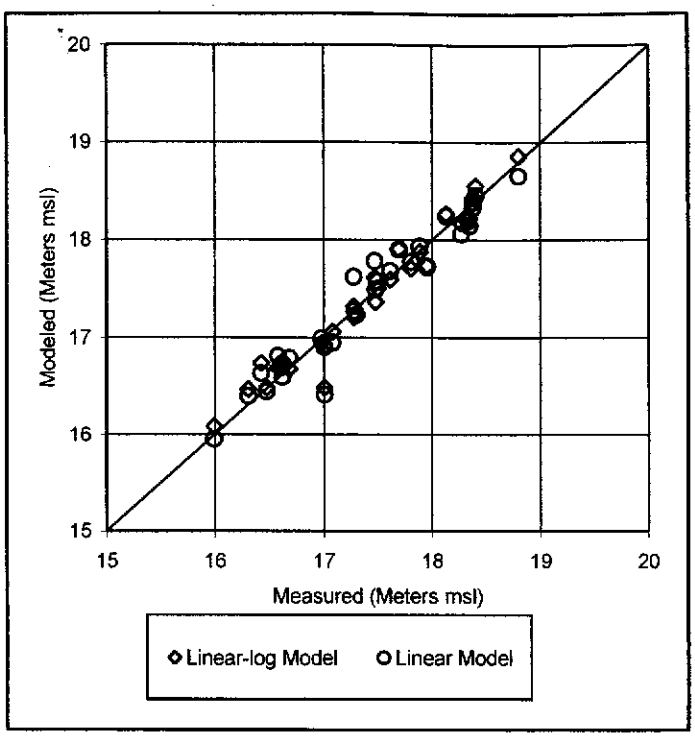

Figure 15. Measured versus modeled water level from the jackknifing analysis.

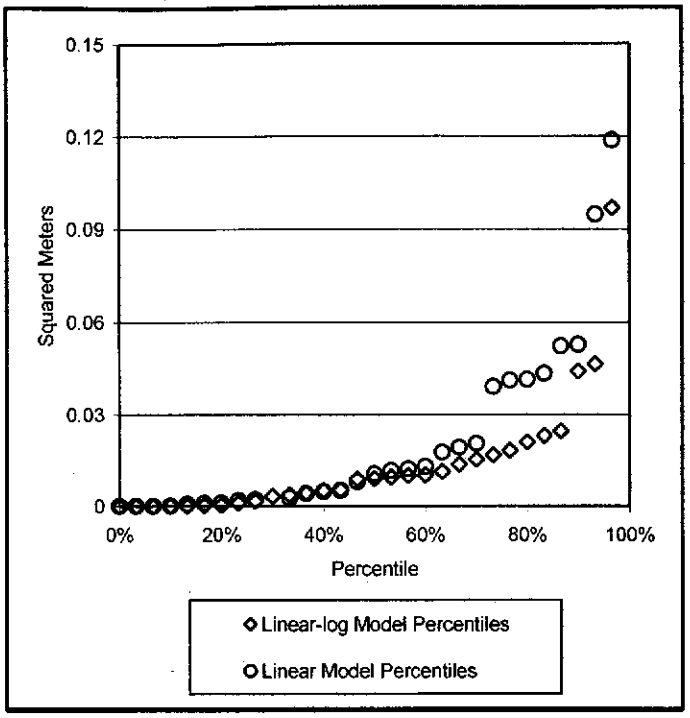

Figure 16. Percentile plot of squared residuals from the jackknifing analysis.

ogram is linear at low lag distances. The commonly cited log-normal approximation for the distribution of many hydrogeologic properties, such as hydraulic conductivity (Roth 1998), might suggest an exponential semivariogram is also an appropriate selection. However, experimentation with a number of different water-level datasets kriged using the linear-log drift model and various residual semivariograms suggests that, typically, linear and spherical semivariograms produce maps that describe the data satisfactorily and quickly return to the drift outside the convex data domain. For purposes of this study, the maps used for the particle-tracking exercise mentioned were created in a single kriging step using a default linear semivariogram; however, the authors suggest that appropriate semivariogram selection and fitting should be conducted as part of any rigorous study of ground water level data.

Jackknife Model Comparison

The uncertainty related to kriging approaches (or models) is often assessed by mapping the kriging standard deviations and/or the Lagrange multipliers. These are intimately related to the modeled semivariogram parameters, i.e., the sill, nugget, and range, and are not directly influenced by the form of drift model used. The form of the kriging equation (Equation 1) can be considered as two "stacked" models, i.e., the expression representing the drift term, and an expression (or series of nested expressions) representing the residual semivariogram. The linear-log drift approach represents a revision of the drift term (m[u]) and does not directly affect the methodologies for modeling of the residual (R[u]) component, which in either the linear-log or linear case is modeled as a single or series of stacked analytical approximations to the calculated semivariogram. Ideally, of course, if a "better" drift model is used, the calculated residuals may be smaller, resulting in a smaller variance and smaller kriging standard deviations. However, semivariogram modeling can be a subjective exercise, and comparison of kriging standard deviations and/or Lagrange multipliers includes this

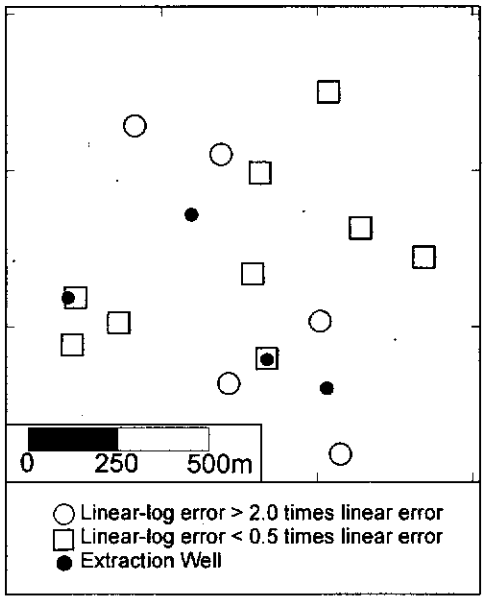

Figure 17. Map of relative error from the jackknifing analysis.

subjectivity. For this reason, the authors have attempted in the following to present a concise comparative analysis of model errors arising from the linear-log and linear drifts alone (i.e., errors related to modeling the m[u] term) and avoid a discussion of errors related to semivariogram modeling.

Numerous methods of varying complexity are available to assess or compare the correctness of model structure. Principal among these in geostatistics is jackknifing (or single-point cross-validation). In this method, each data point is, in turn, suppressed (removed from the dataset) and estimated using the kriging model based on the remaining data. The differences between the measured value and estimated values can be squared and summed, and this value used to indicate the accuracy of the model. This approach has

been used to compare the linear-log and linear-drift models, by estimating the value of the drift component of Equation 1 at each suppressed point, in turn, and summing the squared differences. The calculated sum-of-squared differences are 0.67 and 0.97 m^2 for the linear-log and linear-drift models, respectively. The scattergram (Figure 15) and rank-percentile plot (Figure 16) further support the conclusion that the linear-log drift model is a better model, or predictor, of the measured water levels.

As outlined in Gaganis and Smith (2001), errors arising from the imperfect mathematical representation of the structure of a hydrologic system, i.e., model error, are not random but rather systematic. A review of model error may elucidate the form of this systematic error, or model bias. For the Cape Cod dataset, the squared residuals calculated from the jackknifing approach have been mapped in Figure 17. Where data are available adjacent to the extraction wells, the linear-log error is less than half the linear error (indicated by a square); away from the extraction wells, the pattern appears more random. This simple comparison supports the intuitive conclusion that residuals from the linear-drift model are biased high adjacent to the extraction wells, where the form of the drift model is unable to represent the shape of the depressed potentiometric surface.

Further analysis of the residuals might indicate that their magnitude and distribution reflect deviations of field conditions from the assumptions implicit in the linear-log drift model, such as aquifer homogeneity, isotropy, and well penetration. If hydraulic conductivity data are available throughout the modeled domain on a frequency equal to or greater than that of water-level data, cokriging the water levels with colocated hydraulic conductivity data (Deutsch and Journel 1998) might indicate the distribution of error is correlated to hydraulic conductivity by reducing overall error.

Parameter Estimation

Although a priori knowledge of aquifer properties such as transmissivity (T) and storage coefficient (S) is not required or explicitly included within the kriging routine presented, knowledge of these properties from long-term pumping tests provide valuable means of verifying, for example, capture zones calculated using the kriged ground water surface. By restructuring the linear-log drift with the explicit inclusion of T, it should be possible to elucidate the optimum value of T matching the measured data. This possibility suggests a potential for linear-log kriging as a parameter estimation procedure, although this has not been investigated by the authors at this time.

Conclusions

The purpose of this paper is to introduce a simple, single-step kriging routine that improves on existing methods used with two-dimensional water-level data. The linear-log kriging approach was developed as a practical solution to improving the level of interpretation possible from measured ground water level data. Providing that violations of the assumptions accompanying the Theis approximation are limited, application of the method described herein provides a gridded ground water surface suitable for tracking particles to estimate well-capture zones. The surface created comes closer to conserving flow than when a linear drift is used. Preliminary estimates of well capture can be made within moments of water-level measurement. For an ideal homogeneous, isotropic aquifer with fully penetrating wells, the gridded surface may be considered as a calibrated, two-dimensional model of the potentiometric surface. In cases where these limiting assumptions are fairly well adhered to, consideration of the effort and accuracy of numerical modeling (versus the method described) might indicate the latter to be a more cost-beneficial approach to estimating plume capture. Additional potential exists for a single-step estimation of aquifer transmissivity.

Acknowledgments

The authors wish to thank the Air Force Center for Environmental Excellence (AFCEE), Massachusetts Military Reservation, Cape Cod, for releasing the dataset used in this study, and to Michael Karlinger for advice and insights into kriging theory.

The authors wish to thank the reviewers for their insightful comments: In particular, those of Greg McNulty prompted the jackknifing analysis that solidified the manuscript.

Further Information

Copies of the compiled FORTRAN and Visual Basic executables used in preparation of this report are available by contacting Matthew Tonkin at the address provided.

References

Air Force Center for Environmental Excellence (AFCEE). 2000. Comprehensive long-term monitoring plan, version 1.0., August 2000. Prepared for AFCEE/MMR Installation Restoration Program by Jacobs Engineering Group Inc.

Chiles, J.P., and P. Delfiner. 1999. *Geostatistics—Modeling Spatial Uncertainty*. New York: John Wiley and Sons.

Clark, I., and W.V. Harper. 2000. *Practical Geostatistics 2000*. Columbus, Ohio: Ecosse North America Llc.

Delhomme, J.P. 1978. Kriging in the hydrosciences. *Advances in Water Resources* 1, no. 5: 252-266.

Deutsch, C.V., and A.G. Journel. 1998. *GSLIB: Geostatistical Software Library and User's Guide*, 2nd edition. New York: Oxford University Press.

Ferris, J.G., D.B. Knowles, R.H. Brown, and R.W. Stallman. 1962. Theory of aquifer tests. U.S. Geological Survey Water-Supply Paper 1536-E.

Gaganis, P., and L. Smith. 2001. A bayesian approach to the quantification of the effect of model error on the predictions of ground water models. *Water Resources Research* 37, no. 9: 2309-2322.

Hess, K.M., S.H. Wolf, and M.A. Celia. 1992. Large scale natural gradient tracer test in sand and gravel, Cape Cod, Massachusetts: 3. Hydraulic conductivity variability and calculated macrodispersivities. *Water Resources Research* 28, no. 8: 2011-2027.

Rouse, H. (ed.) 1949. *Engineering Hydraulics: Proceedings of the Fourth Hydraulics Conference*, Iowa Institute of Hydraulic Research, June 12-15, 1949.New York: John Wiley and Sons.

Roth, C. 1998. Is lognormal kriging suitable for local estimation? *Mathematical Geology* 30, no. 8: 999-1009.

Skrivan, J.A., and M.R. Karlinger. 1977. Semi-variogram estimation and universal kriging program, Program Number K603. Tacoma, Washington: U.S. Geological Survey Water Resources Division.

Volpi, G., and G. Gambolati. 1978. On the use of a main trend for the kriging technique in hydrology. *Advances in Water Resources* 1, 345–349.

Zheng, C. 1992. Path3D 3.2: *A Ground-Water Path and Travel-Time Simulator.* Bethesda, Maryland: S.S. Papadopulos and Associates.

Zheng, C. 1994. Analysis of particle tracking errors associated with spatial discretization. *Ground Water* 32, no. 5: 821-828.